Impulse Noise Removal by Median-type Noise Detectors and Edge-preserving Regularization

by

HO Chung Wa

A Thesis Submitted in Partial Fulfillment
of the Requirements for the Degree of
Master of Philosophy
in
Mathematics

July 2004

Abstract

Abstract of thesis entitled:

Impulse Noise Removal by Median-type Noise Detectors and Edge-preserving Regularization

Submitted by HO Chung Wa

for the degree of Master of Philosophy in Mathematics

at The Chinese University of Hong Kong in July 2004

This thesis proposes a two-phase scheme for impulse noise removal. In the first phase, an adaptive median filter, or other common median-type filters, is used to identify pixels which are likely to be contaminated by noise (noise candidates). In the second phase, the image is restored using a specialized regularization method that applies only to those selected noise candidates. In terms of edge preservation and noise suppression, the restored images show a significant improvement compared to those restored by using just nonlinear filters or regularization methods only.

From the computational aspect, the second phase is equivalent to solving a one-dimensional nonlinear equation for each noise candidate. One can solve these equations by using Newton's method. However, because of the edge-preserving term, the domain of convergence of Newton's method will be very narrow. To overcome the difficulty, the initial guesses will be derived for these equations such that Newton's method will always converge.

The thesis is based on the following two papers, which will be referred to in the text by Paper I and Paper II.

Paper I. [4] R. H. Chan, C.-W. Ho, and M. Nikolova, "Salt-and-pepper noise removal by median-type noise detectors and edge-preserving regu-

larization," submitted to *IEEE Transactions of Image Processing.*

Paper II. [5] R. H. Chan, C.-W. Ho, and M. Nikolova, "Convergence of Newton's method for a minimization problem in impulse noise removal," *Journal of Computational Mathematics*, 2 (2004), pp. 168–177.

摘要

香港中文大學碩士論文摘要

論文題目：

使用具中值特性的檢波器及具邊界保存性的正則化方法去除脈衝噪聲

何仲華

二零零四年六月

本論文提出去除脈衝噪聲的二階段法。在第一階段，適應中值濾波，或其他具有中值特性的常用濾波，會用作辨認可能受噪聲干擾的像素（稱為疑似噪聲）。在第二階段，向疑似噪聲運用特別的正則化方法，把圖像復原。從復原圖像中的細節保存及噪聲壓抑兩方面，我們提出的二階段法比只利用非線性濾波或正則化方法得出的復原圖像有明顯的改善。

算法方面，在二階段法中的第二階段，壓抑每一個疑似噪聲是等同求對應的一維非線性方程的解。牛頓法當然可以用來解這些方程；但是，受制於正則化方法的邊界保存項，牛頓法的的收斂域是非常小的。要克服這個困難，我們要導出令牛頓法收斂的初始值。

論文是根據以下兩篇文章寫成，在文中分別被引為文章一及文章二：

文章一 [4] R. H. Chan, C.-W. Ho, and M. Nikolova, "Salt-and-pepper noise removal by median-type noise detectors and edge-preserving regularization," submitted to *IEEE Transactions of Image Processing.*

文章二 [5] R. H. Chan, C.-W. Ho, and M. Nikolova, "Convergence of Newton's method for a minimization problem in impulse noise removal," *Journal of Computational Mathematics*, 2 (2004), pp. 168–177.

ACKNOWLEDGMENTS

I wish to express my sincere and deepest gratitude to my supervisor, Prof. Raymond H. F. Chan, for his inspired guidance, constant encouragement and help throughout the period of my M. Phil. studies and in the preparation of this thesis.

Moreover, I am deeply grateful to Dr. Mila Nikolova of the Centre de Mathématiques et de Leurs Applications for her invaluable comments and suggestions in preparation of the papers and careful reading of this thesis.

Finally, I would like to thank all my academic brothers — Mr. Z. J. Bai, Mr. C. Hu, Mr. K. T. Ling, Mr. K. C. Ma, Mr. Y. H. Tam, Mr. C. Y. Wong and Mr. Y. S. Wong for their very helpful discussions.

Contents

Introduction

Denoising is an important topic in image processing. When an image is converted from one form to another or transmitted through a channel, different types of noise could be present in the image. For example, Gaussian noise in digital images arise during image acquisition with a CCD camera, impulse noise arise when pixel values are quantized to binary bits and transmitted in a noisy link. As a result, any further enhancement of noisy images, such as deblurring, segmentation, edge detection, etc., may not be performed in resulting images. In this thesis, removal of impulse noise is focused.

Impulse noise is caused by malfunctioning pixels in camera sensors, faulty memory locations in hardware, or transmission in a noisy channel, see [3] for reference. In this model, only a portion of pixels, but not all, in an image will be corrupted as white and black dots superimposed on an image. This is a contrast to Gaussian noise where every pixel in the original image will be perturbed a little bit, see Figure 1 for the comparison. There are many works proposed to restore images corrupted by impulse noise, such as the nonlinear digital filters reviewed in [1]. Because of good denoising power and computational efficiency, the median filter was once the most popular nonlinear filter for removing impulse noise [3, 9]. The denoising principle of median filter is to replace the current pixel by the median of neighboring pixel values. However, it has been shown in [12] that when the proportion of the noise is over 50%, the details, edges and features

(a) (b) (c)

Figure 1: (a) The original image. (b) The image corrupted by impulse noise. (c) The image corrupted by Gaussian noise.

of the original image are jittered by the filter.

Different remedies of the median filter have been proposed to overcome the drawback, e.g. the adaptive median filter [10], the multi-state median filter [8]. The idea is to identify possible noise pixels first and then to replace the detected noisy pixels by using the median filter or its variants, while leaving all other pixels unchanged. All these filters are good in detecting the noise even at a high noise level, but the shortcoming is that the noisy pixels are replaced by some median values over their vicinity, without taking into account local features such as the possible presence of edges. Hence details and edges are not recovered satisfactorily, especially when the noise level is high.

For images corrupted by Gaussian noise, the regularized least-squares methods, based on edge-preserving regularization functionals [2, 6, 7, 13] have been used successfully to preserve the edges and the details in the images. In this method, the restored image, denoted by $\mathbf{x}$, will solve the minimization problem:

$$\min_{\mathbf{x}} \|\mathcal{A}\mathbf{x} - \mathbf{y}\|_2^2 + \beta \cdot \mathcal{R}(\mathbf{x}). \tag{1}$$

Here $\mathbf{y}$ is an observed noisy image, $\mathcal{A}$ is a known linear blur operator (usually a convolution operator) arising from the modelling of image formulation. If it is

a denoising problem, $\mathcal{A}$ will be taken as an identity operator $\mathcal{I}$. Then the data-fidelity term, or data-fitting term, $\|\mathcal{A}\mathbf{x}-\mathbf{y}\|_2^2$ measures the closeness between the observed image and the restored image, while $\mathcal{R}$ is an edge-preserving operator which measures the smoothness of the restored image. And β is the regularization parameter which controls the tradeoff between the data-fidelity and the regularity of $\mathbf{x}$.

Above formulation fails in the presence of impulse noise because of ℓ_2-norm in data-fidelity term, and then when the impulse noise is smoothed, all pixels in the image, including those pixels which are not corrupted by the impulse noise, will be altered. To avoid such problem, the modified minimization formulation

$$\min_{\mathbf{x}} \|\mathbf{x}-\mathbf{y}\|_1 + \beta \cdot \mathcal{R}(x), \tag{2}$$

is proposed to deal with impulse noise [11]. The critical change from smooth ℓ_2-norm to non-smooth ℓ_1-norm in data-fidelity term results in a different aspect of the regularization method. In formulation (1), the restored image $\mathbf{x}$ and the observed image $\mathbf{y}$ is close, but all pixels, including uncorrupted ones, are still perturbed, and this perturbation is sensitive to the impulse noise. On the other hand, there is no such phenomenon in formulation (2). This means that except for some uncorrupted pixels, most impulse noise (no matter how large the pixel intensity is) will be removed and restored to fit the features of the image. In other words, most uncorrupted pixels are fitted exactly while the outliers are removed. This formulation is well-suited to the denoising problem.

However, when the noise level is high, the corrupted noise pixels will be connected and formed as neighbors, and appeared as patches of noise. These will be called as 'noise patches'. In order to smooth out such noise patches, one should increase the regularization parameter β in (2). Consequently, pixels at the edges of an image will be unavoidably altered too. As a result, removal of noise patches will be a difficult task in denoising problem. To overcome the drawback, a pow-

erful two-phase scheme which combines the variational method proposed in [11], i.e., the formation (2), with the adaptive median filter [10] is proposed in Paper I [4]. Denoting $\mathbf{x} = \{x_i\}$ and $\mathbf{y} = \{y_i\}$, the resulting formulation is to solve

$$\begin{cases} \min\limits_{\mathbf{x}} \sum\limits_{i} |x_i - y_i| + \beta \sum\limits_{i} \sum\limits_{j \in \mathcal{V}_i} \varphi(x_i - x_j), \\ \text{subject to} \quad x_i = y_i \quad \text{if } i \notin \mathcal{N}, \end{cases} \tag{3}$$

where φ is an edge-preserving function which preserves the edges of an image by considering the neighboring pixels x_j, $j \in \mathcal{V}_i$, of x_i, and $\mathcal{N}$ is a noise candidate set obtained from adaptive median filter. This means if a pixel y_j is detected by the filter as noise, i.e. $j \in \mathcal{N}$, this pixel will be considered as a noise candidate. The constrained minimization approach is much better than just using either the variational method or the adaptive median filter only. In particular, salt-and-pepper noise with noise ratio as high as 90% can be cleaned quite efficiently.

From the computational aspect, solving (3) is equivalent to solving a system of nonlinear equations for the pixels in an image. As shown in [11], the root finding can be done by relaxation method, and it results in solving a one-dimensional nonlinear equation for each noise candidate in $\mathcal{N}$. However, the presence of the edge-preserving regularization term introduces difficulties in solving the equations because the highly nonlinear functions involving φ can have very large derivatives in some regions, see Figure 2. In particular, the convergence domain can be very

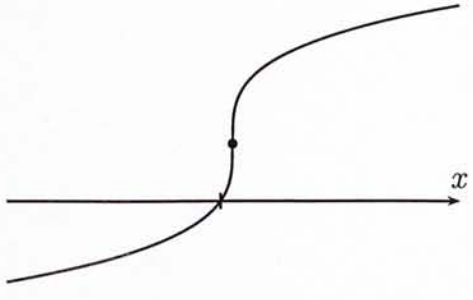

Figure 2: The resulting nonlinear equation that has to be solved.

small if Newton's method is adopted. As a result, an algorithm is developed in Paper II [5] to locate the initial guess such that Newton's method always converges.

References

[1] J. Astola and P. Kuosmanen, *Fundamentals of Nonlinear Digital Filtering.* Boca Raton, CRC, 1997.

[2] C. Bouman and K. Sauer, "On discontinuity-adaptive smoothness priors in computer vision," *IEEE Transactions on Pattern Analysis and Machine Intelligence*, 17 (1995), pp. 576–586.

[3] A. Bovik, *Handbook of Image and Video Processing*, Academic Press, 2000.

[4] R. H. Chan, C.-W. Ho, and M. Nikolova, "Salt-and-pepper noise removal by median-type noise detectors and edge-preserving regularization," submitted to *IEEE Transactions of Image Processing.*

[5] R. H. Chan, C.-W. Ho, and M. Nikolova, "Convergence of Newton's method for a minimization problem in impulse noise removal," *Journal of Computational Mathematics*, 2 (2004), pp. 168–177.

[6] T. F. Chan, H. M. Zhou, and R. H. Chan, "A continuation method for total variation denoising problems," *Proceedings of SPIE Symposium on Advanced Signal Processing: Algorithms, Architectures, and Implementations, ed. F. T. Luk*, 2563 (1995), pp. 314–325,

[7] P. Charbonnier, L. Blanc-Féraud, G. Aubert, and M. Barlaud, "Deterministic edge-preserving regularization in computed imaging," *IEEE Transactions on Image Processing*, 6 (1997), pp. 298–311.

[8] T. Chen and H. R. Wu, "Space variant median filters for the restoration of impulse noise corrupted images," *IEEE Transactions on Circuits and Systems II*, 48 (2001), pp. 784–789.

[9] T. S. Huang, G. J. Yang, and G. Y. Tang, "Fast two-dimensional median filtering algorithm," *IEEE Transactions on Acoustics, Speech, and Signal Processing*, 1 (1979), pp. 13–18.

[10] H. Hwang and R. A. Haddad, "Adaptive median filters: new algorithms and results," *IEEE Transactions on Image Processing*, 4 (1995), pp. 499–502.

[11] M. Nikolova, "A variational approach to remove outliers and impulse noise," *Journal of Mathematical Imaging and Vision*, 20 (2004), pp. 99–120.

[12] T A. Nodes and N. C. Gallagher, Jr. "The output distribution of median type filters," *IEEE Transactions on Communications*, COM-32, 1984.

[13] C. R. Vogel and M. E. Oman, "Fast, robust total variation-based reconstruction of noisy, blurred images," *IEEE Transactions on Image Processing*, 7 (1998), pp. 813–824.

Paper I: Salt-and-Pepper Noise Removal by Median-type Noise Detectors and Edge-preserving Regularization *

Abstract

This paper proposes a two-phase scheme for removing salt-and-pepper impulse noise. In the first phase, an adaptive median filter is used to identify pixels which are likely to be contaminated by noise (noise candidates). In the second phase, the image is restored using a specialized regularization method that applies only to those selected noise candidates. In terms of edge preservation and noise suppression, our restored images show a significant improvement compared to those restored by using just nonlinear filters or regularization methods only. Our scheme can remove salt-and-pepper-noise with noise level as high as 90%.

Keywords. Impulse noise, adaptive median filter, edge-preserving regularization.

1 Introduction

Impulse noise is caused by malfunctioning pixels in camera sensors, faulty memory locations in hardware, or transmission in a noisy channel, see [4] for reference.

*Paper I is a joint work with Raymond H. Chan and Mila Nikolova.

There are mainly two types of impulse noise: salt-and-pepper noise and random-valued noise. For images corrupted by salt-and-pepper noise, the noisy pixels can take only the maximum and the minimum values in the dynamic range. In contrast, the noisy pixels in images corrupted by random-valued noise can take any random values in the dynamic range. In this paper, we propose a method for recovering images corrupted by salt-and-pepper noise with noise ratio as high as 90%.

There are many works proposed to restore images corrupted by impulse noise, see for instance the nonlinear digital filters reviewed in [1]. The median filter was once the most popular nonlinear filter for removing impulse noise, especially the salt-and-pepper noise, because of its good denoising power [4] and computational efficiency [14]. However, it has been shown in [18] that when the noise level is over 50%, the details and edges of the original image are jittered by the filter.

Different remedies of the median filter have been proposed, e.g. the adaptive median filter [15], the multi-state median filter [9], or the median filter based on homogeneity information [10, 19]. The idea is to identify possible noise pixels first and then to replace only the detected noisy pixels by using the median filter or its variants, while leaving all other pixels unchanged. This is why these filters are said to be "decision-based" or "switching". All these filters are good in *detecting* the noise even at a high noise level, but the main drawback is that the noisy pixels are replaced by some median values over their vicinity, without taking into account local features such as the possible presence of edges. Hence details and edges are not recovered satisfactorily, especially when the noise level is high.

For images corrupted by Gaussian noise, regularized least-squares methods, based on edge-preserving regularization functionals [3, 6, 8, 20] have been used successfully to preserve the edges and the details in the images. These methods fail in the presence of impulse noise because the noise is heavy tailed, and the restoration will alter considerable amount of pixels in the image, including those pixels which are not corrupted by the impulse noise. Recently, non-smooth data-

fidelity terms (e.g. ℓ_1) have been used along with edge-preserving regularization to deal with impulse noise [17].

In this paper, we propose a powerful two-stage scheme which combines the variational method proposed in [17] with the adaptive median filter [15]. More precisely, the noise candidates are first identified by the adaptive median filter, and then these noise candidates are selectively restored using an objective function with an ℓ_1 data-fitting term and an edge-preserving regularization term. Since the edges are preserved for the noise candidates, and no changes are made to the pixels that are not the noise candidates, the performance of our combined approach is much better than just using either one of the methods. Salt-and-pepper noise with noise ratio as high as 90% can be cleaned quite efficiently.

The outline of the paper is as follows. Review of the adaptive median filter and the edge-preserving method are described in Section 2. Our denoising scheme is presented in Section 3. Experimental results and conclusions are presented in Sections 4 and 5 respectively.

2 Adaptive median filter and edge-preserving regularization

2.1 Review of the adaptive median filter

Let $x_{i,j}$, for $(i,j) \in \mathcal{A} \equiv \{1,\ldots,M\} \times \{1,\ldots,N\}$, be the gray level of a true M-by-N image $\mathbf{x}$ at pixel location (i,j), and $[s_{\min}, s_{\max}]$ be the dynamic range of $\mathbf{x}$. Denote $\mathbf{y}$ a noisy image. In the classical "salt-and-pepper" impulse noise model, the observed gray level at pixel location (i,j) is given by

$$y_{i,j} = \begin{cases} s_{\min}, & \text{with probability } p, \\ s_{\max}, & \text{with probability } q, \\ x_{i,j}, & \text{with probability } 1-p-q, \end{cases}$$

where $r = p + q$ defines the noise level. Here we give a brief review of the filter.

Let $S_{i,j}^w$ be a window of size $w \times w$ centered at (i, j), i.e.

$$S_{i,j}^w = \{(k, l) \ : \ |k - i| \leq w \text{ and } |j - l| \leq w\}$$

and let $w_{\max} \times w_{\max}$ be the maximum window size. The algorithm tries to identify the noise candidates $y_{i,j}$, and then replace each $y_{i,j}$ by the median of the pixels in $S_{i,j}^w$.

Algorithm I (Adaptive Median Filter)

For each pixel location (i, j), do

1. Initialize $w = 3$.
2. Compute $s_{i,j}^{\min,w}$, $s_{i,j}^{\text{med},w}$ and $s_{i,j}^{\max,w}$, which are the minimum, median and maximum of the pixel values in $S_{i,j}^w$ respectively.
3. If $s_{i,j}^{\min,w} < s_{i,j}^{\text{med},w} < s_{i,j}^{\max,w}$, then go to Step 5. Otherwise, set $w = w + 2$.
4. If $w \leq w_{\max}$ go to Step 2. Otherwise, we replace $y_{i,j}$ by $s_{i,j}^{\text{med},w_{\max}}$.
5. If $s_{i,j}^{\min,w} < y_{i,j} < s_{i,j}^{\max,w}$, then $y_{i,j}$ is not a noise candidate, else we replace $y_{i,j}$ by $s_{i,j}^{\text{med},w}$.

The adaptive structure of the filter ensures that most of the "salts" and "peppers" are detected even at a high noise level provided that the window size is large enough. Notice that the noise candidates are replaced by the median $s_{i,j}^{\text{med},w}$, while the remaining pixels are left unaltered.

2.2 Variational method for impulse noise cleaning

In [17], impulse noise corrupted images are restored by minimizing a convex objective function $F_{\mathbf{y}} : \mathbb{R}^{M \times N} \to \mathbb{R}$ of the form

$$F_{\mathbf{y}}(\mathbf{u}) = \sum_{(i,j) \in \mathcal{A}} |u_{i,j} - y_{i,j}| + \frac{\beta}{2} \sum_{(i,j) \in \mathcal{A}} \sum_{(m,n) \in \mathcal{V}_{i,j}} \varphi(u_{i,j} - u_{m,n}), \tag{1}$$

where $\mathcal{V}_{i,j}$ is the set of the four closest neighbors of (i,j), not including (i,j). It was shown in [16] and [17] that under mild assumptions and a pertinent choice of β, the minimizer $\hat{\mathbf{u}}$ of $F_{\mathbf{y}}$ ensures that $\hat{u}_{i,j} = y_{i,j}$ for most of the uncorrupted pixels $y_{i,j}$. Furthermore, all pixels $\hat{u}_{i,j}$ such that $\hat{u}_{i,j} \neq y_{i,j}$ are restored so that edges and local features are well preserved, provided that φ is an edge-preserving potential function. Examples of such functions are:

$$\varphi(t) = \sqrt{\alpha + t^2}, \quad \alpha > 0,$$
$$\varphi(t) = |t|^{\alpha}, \quad 1 < \alpha \leq 2,$$

see [2, 3, 8, 12]. The minimization algorithm works on the residuals $\mathbf{z} = \mathbf{u} - \mathbf{y}$. It is sketched below:

Algorithm II

1. Initialize $z_{ij}^{(0)} = 0$ for each $(i,j) \in \mathcal{A}$.

2. At each iteration k, calculate, for each $(i,j) \in \mathcal{A}$,

$$\xi_{i,j}^{(k)} = \beta \sum_{(m,n)\in\mathcal{V}_{i,j}} \varphi'(y_{i,j} - z_{m,n} - y_{m,n}),$$

   where $z_{m,n}$, for $(m,n) \in \mathcal{V}_{i,j}$, are the latest updates and φ' is the derivative of φ.

3. If $\left|\xi_{i,j}^{(k)}\right| \leq 1$, set $z_{i,j}^{(k)} = 0$. Otherwise, solve for $z_{i,j}^{(k)}$ in the nonlinear equation

$$\beta \sum_{(m,n)\in\mathcal{V}_{i,j}} \varphi'(z_{i,j}^{(k)} + y_{i,j} - z_{m,n} - y_{m,n}) = \operatorname{sign}(\xi_{i,j}^{(k)}). \tag{2}$$

The updating of $z_{i,j}^{(k)}$ can be done in a red-black fashion, and it was shown in [17] that $\mathbf{z}^{(k)}$ converges to $\hat{\mathbf{z}} = \hat{\mathbf{u}} - \mathbf{y}$, where the restored image $\hat{\mathbf{u}}$ minimizes $F_{\mathbf{y}}$ in (1). If we choose $\varphi(t) = |t|^{\alpha}$, the nonlinear equation (2) can be solved by Newton's method with quadratic convergence by using a suitable initial guess derived in [5].

3 Our method

Many denoising schemes are switching median filters, see for example, [9, 10, 22]. This means that the noise candidates are first detected by some rules and then replaced by the median output or its variants. For instance, in Algorithm I, the noise candidate $y_{i,j}$, $(i,j) \in \mathcal{N}$, is replaced by $s_{i,j}^{\text{med},w}$. Switching schemes are a good approach because the uncorrupted pixels will not be modified. However, the replacement methods in these denoising schemes cannot preserve the features of the images, in particular the edges are jittered.

In contrast, Algorithm II can preserve edges during denoising but it has problem in detecting noise patches, i.e., when many noise pixels are connecting with each other. If one wishes to smooth out all the noise patches, one has to increase β, see [7] for the role of β. As a result, some signal pixels at the edges will be distorted.

Combining both methods will avoid the drawbacks of either one of them. Replacing the noise pixels with the correct one and keeping the edge is the aim of our method. In the following, we denote the restored image by $\hat{\mathbf{x}}$.

Algorithm III

1. *(Noise detection):* Denote $\tilde{\mathbf{y}}$ the image obtained by applying an adaptive median filter to the noisy image $\mathbf{y}$. Noticing that noisy pixels take their values in the set $\{s_{\min}, s_{\max}\}$, we define the noise candidate set as

$$\mathcal{N} = \{(i,j) \in \mathcal{A} : \tilde{y}_{i,j} \neq y_{i,j} \text{ and } y_{i,j} \in \{s_{\min}, s_{\max}\}\}.$$

   The set of all uncorrupted pixels is $\mathcal{N}^c = \mathcal{A} \setminus \mathcal{N}$.

2. *(Replacement):* Since all pixels in $\mathcal{N}^c$ are detected as uncorrupted, we naturally keep their original values, i.e., $\hat{x}_{i,j} = y_{i,j}$ for all $(i,j) \in \mathcal{N}^c$. Let us now consider a noise candidate, say corresponding to $(i,j) \in \mathcal{N}$. Each one of its neighbors $(m,n) \in \mathcal{V}_{i,j}$ is either a correct pixel, i.e., $(m,n) \in \mathcal{N}^c$ and hence

$\hat{x}_{m,n} = y_{m,n}$; or is another noise candidate, i.e., $(m,n) \in \mathcal{N}$, in which case its value must be restored. The neighborhood $\mathcal{V}_{i,j}$ of (i,j) is thus split as $\mathcal{V}_{i,j} = (\mathcal{V}_{i,j} \cap \mathcal{N}^c) \cup (\mathcal{V}_{i,j} \cap \mathcal{N})$. Noise candidates are restored by minimizing a functional of the form (1), but restricted to the noise candidate set $\mathcal{N}$:

$$F_{\mathbf{y}}|_{\mathcal{N}}(\mathbf{u}) = \sum_{(i,j)\in\mathcal{N}} \left[|u_{i,j} - y_{i,j}| + \frac{\beta}{2}(S_1 + S_2) \right] \tag{3}$$

where

$$S_1 = \sum_{(m,n)\in\mathcal{V}_{i,j}\cap\mathcal{N}^c} \varphi(u_{i,j} - y_{m,n}),$$

$$S_2 = \sum_{(m,n)\in\mathcal{V}_{i,j}\cap\mathcal{N}} \varphi(u_{i,j} - u_{m,n}).$$

The restored image $\hat{\mathbf{x}}$ with indices $(i,j) \in \mathcal{N}$ is the minimizer of (3) which can be obtained by using Algorithm II but restricted onto $\mathcal{N}$ instead of onto $\mathcal{A}$. As in (1), the ℓ_1 data-fidelity term $|u_{i,j} - y_{i,j}|$ discourages those wrongly detected uncorrupted pixels in $\mathcal{N}$ from being modified to other values. The regularization term $(S_1 + S_2)$ performs edge-preserving smoothing for the pixels indexed by $\mathcal{N}$.

Let us emphasize that Step 1 of our method can be realized by any reliable salt-and-pepper noise detector, such as the multi-state median filter [9] or the improved detector [22], etc. Our choice, the adaptive median filter, was motivated by the fact that it provides a good compromise between simplicity and robust noise detection, especially for high level noise ratios. The pertinence of this choice can be seen from the experimental results in [11] (where the noise level is 50%) or Figures 4(b) and 6(b) (where the noise level is 70%).

4 Simulations

4.1 Configuration

Among the commonly tested 512-by-512 8-bit gray-scale images, the one with homogeneous region (*Lena*) and the one with high activity (*Bridge*) will be selected for our simulations. Their dynamic ranges are $[0, 255]$. In the simulations, tested images will be corrupted by "salt" (with value 255) and "pepper" (with value 0) noise with equal probability. Also a wide range of noise levels varied from 10% to 70% with increment step of 10% will be tested. Restoration performances are quantitatively measured by the peak signal-to-noise ratio (PSNR) and the mean absolute error (MAE) defined in [4, p. 327]:

$$\mathrm{PSNR} = 10 \log_{10} \frac{255^2}{\frac{1}{MN} \sum_{i,j} (r_{i,j} - x_{i,j})^2},$$

$$\mathrm{MAE} = \frac{1}{MN} \sum_{i,j} |r_{i,j} - x_{i,j}|,$$

where $r_{i,j}$ and $x_{i,j}$ denote the pixel values of the restored image and the original image respectively.

For Algorithm I (the adaptive median filter), the maximum window size $w_{\max}$ should be chosen such that it increases with the noise level in order to filter out the noise. Since it is not known a priori, we tried different $w_{\max}$ for any given noise level, and found that $w_{\max}$ given in Table 1 are sufficient for the filtering. We therefore set $w_{\max} = 39$ in all our tests. We remark that with such choice of $w_{\max}$, almost all the salt-and-pepper noise are detected in the filtered images.

For Algorithm II (the variational method in [17]), we choose $\varphi(t) = |t|^\alpha$ as the edge-preserving function. We observe that if α is small ($1 \leq \alpha < 1.1$), most of the noise is suppressed but stair-cases are found at the fine details; and if α is large ($\alpha > 1.5$), the fine details are not distorted seriously but the noise cannot be fully suppressed. The selection of α is a trade-off between the noise suppression and details preservation [17]. In the tests, the best restoration results are not

noise level	$w_{\max} \times w_{\max}$
$r < 25\%$	5×5
$25\% \leq r < 40\%$	7×7
$40\% \leq r < 60\%$	9×9
$60\% \leq r < 70\%$	13×13
$70\% \leq r < 80\%$	17×17
$80\% \leq r < 85\%$	25×25
$85\% \leq r \leq 90\%$	39×39

Table 1: Maximum window size $w_{\max}$ in Algorithm I.

sensitive to α when it is between 1.2 and 1.4. We therefore choose $\varphi(t) = |t|^{1.3}$, and β is tuned to give the best result in terms of PSNR.

For our proposed Algorithm III, the noise candidate set $\mathcal{N}$ should be obtained such that most of the noise are detected. This again amounts to the selection of $w_{\max}$. As mentioned, $w_{\max} = 39$ can be fixed for most purposes. Then we can restore those noise pixels $y_{i,j}$ with $(i,j) \in \mathcal{N}$. As in Algorithm II, the edge-preserving function $\varphi(t) = |t|^{1.3}$ will be used. That leaves only the parameter β to be determined. Later, we will demonstrate that our proposed algorithm is very robust with respect to β and thus we fix $\beta = 5$ in all the tests.

For comparison purpose, Algorithm I, Algorithm II, the standard median (MED) filter, and also recently proposed filters like the progressive switching median (PSM) filter [21], the multi-state median (MSM) filter [9], the noise adaptive soft-switching median (NASM) filter [10], the directional difference-based switching median (DDBSM) filter [13], and the improved switching median (ISM) filter [22] are also tested. For MED filter, the window sizes are chosen for each noise level to achieve its best performance. For MSM filter, the maximum center weights of 7, 5 and 3 are tested for each noise level. For ISM filter, the convolution kernels K_5, K_7 and K_9 and filtering window sizes of 9×9 and 11×11 are

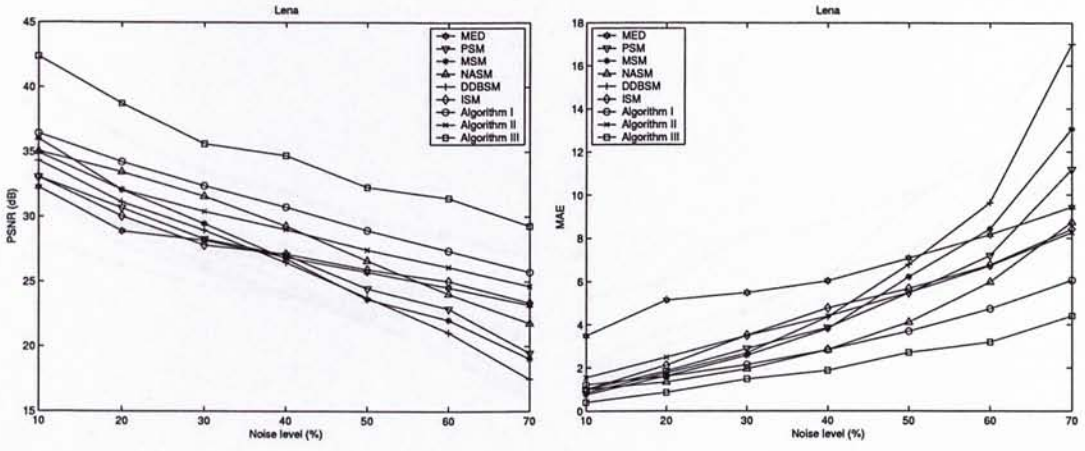

(a) (b)

Figure 1: Results in PSNR and MAE for the *Lena* image at various noise levels for different algorithms.

used. The decision thresholds in PSM, MSM, DDBSM, ISM filters are also tuned to give the best performance in terms of PSNR.

4.2 Denoising Performance

We summarize the performance of different methods in Figures 1 and 2. From the plots, we see that all the methods have similar performance when the noise level is low. This is because those recently proposed methods focus on the noise detection. However when the noise level increases, noise patches will be formed and they may be considered as noise free pixels. This brings difficulties in the noise detection. With erroneous noise detection, no further modifications will be made to the noise patches, and hence their results are not satisfactory.

On the other hand, our proposed denoising scheme achieves a significantly high PSNR and low MAE even when the noise level is high. This is mainly based on the accurate noise detection by the adaptive median filter and the edge-preserving property of the variational method of [17].

In Figures 3 to 6, we present restoration results for the 70% corrupted *Lena*

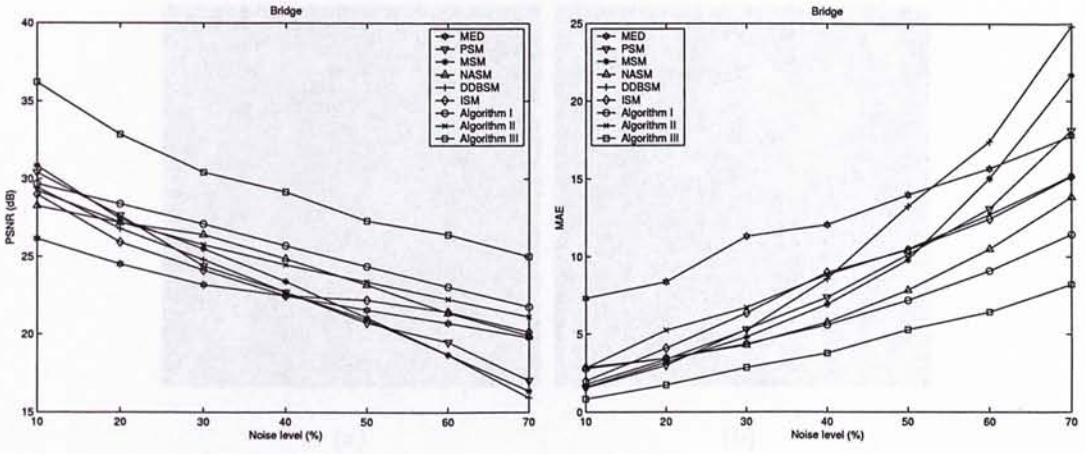

(a) (b)

Figure 2: Results in PSNR and MAE for the *Bridge* image at various noise levels for different algorithms.

and *Bridge* images. Among the restorations, except for our proposed one, Algorithm I gives the best performance in terms of noise suppression and details preservation. As mentioned, it is because the algorithm locates the noise accurately. In fact, about 70.2% and 70.4% pixels are detected as noise candidates in *Lena* and *Bridge* respectively by Algorithm I. However, the edges are jittered by the median filter. For Algorithm II, much of the noise is suppressed but the blurring and distortion are serious. This is because every pixel has to be examined and may have been altered. Compared with all the algorithms tested, our proposed Algorithm III is the best one. It has successfully suppressed the noise with the details and the edges of the images being preserved very accurately.

Finally, to demonstrate the excellent performance of our proposed filter, 90% corrupted *Lena* and *Bridge* are restored by Algorithm I and by our Algorithm III, see Figure 7. We can clearly see the visual differences and also the improvement in PSNR by using our algorithm.

Figure 3: Restoration results of different filters: (a) Corrupted *Lena* image with 70% salt-and-pepper noise (6.7 dB), (b) MED filer (23.2 dB), (c) PSM filter (19.5 dB), (d) MSM filter (19.0 dB), (e) DDBSM filter (17.5 dB), (f) NASM filter (21.8 dB)

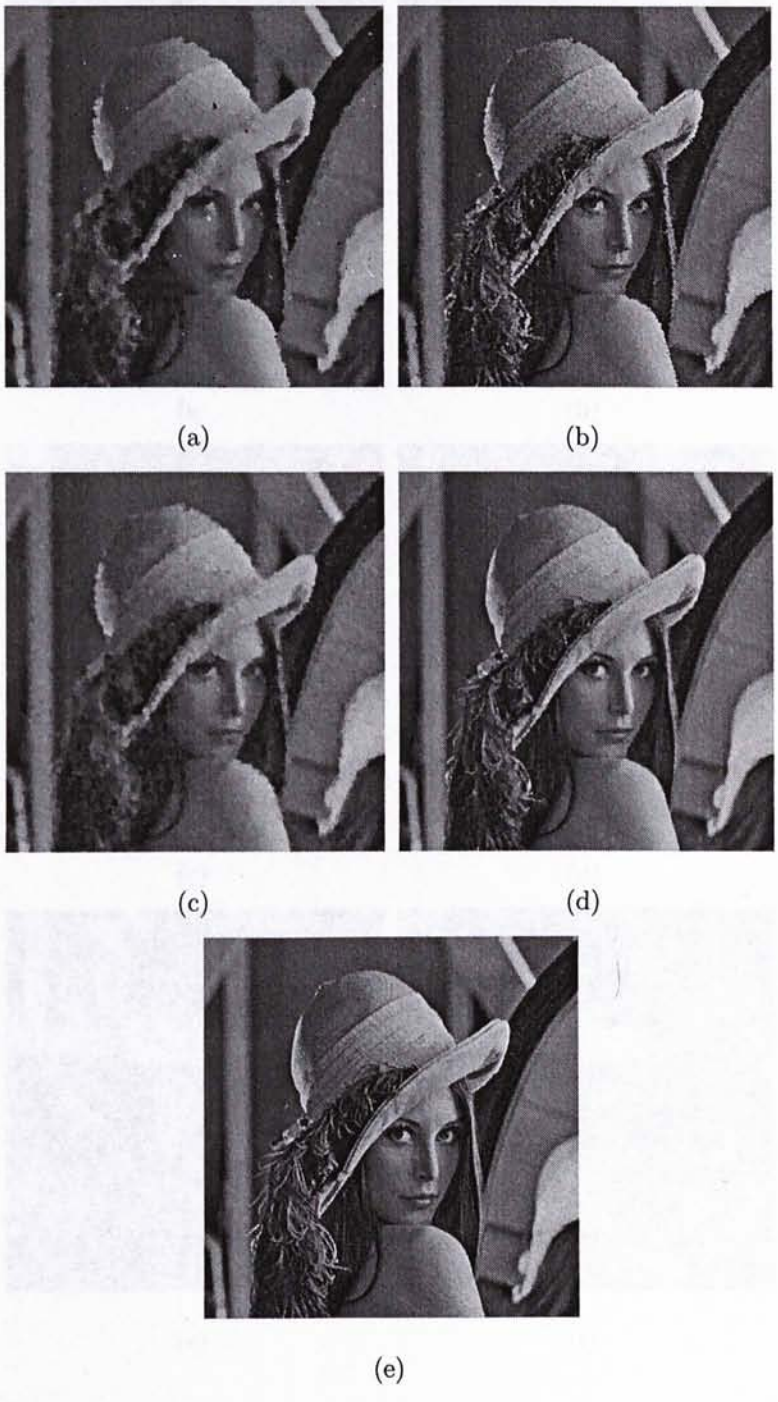

Figure 4: Restoration results of different filters: (a) ISM filter (23.4 dB), (b) Algorithm I (25.8 dB), (c) Algorithm II (24.6 dB), (d) Our proposed algorithm (29.3 dB), and (e) Original image.

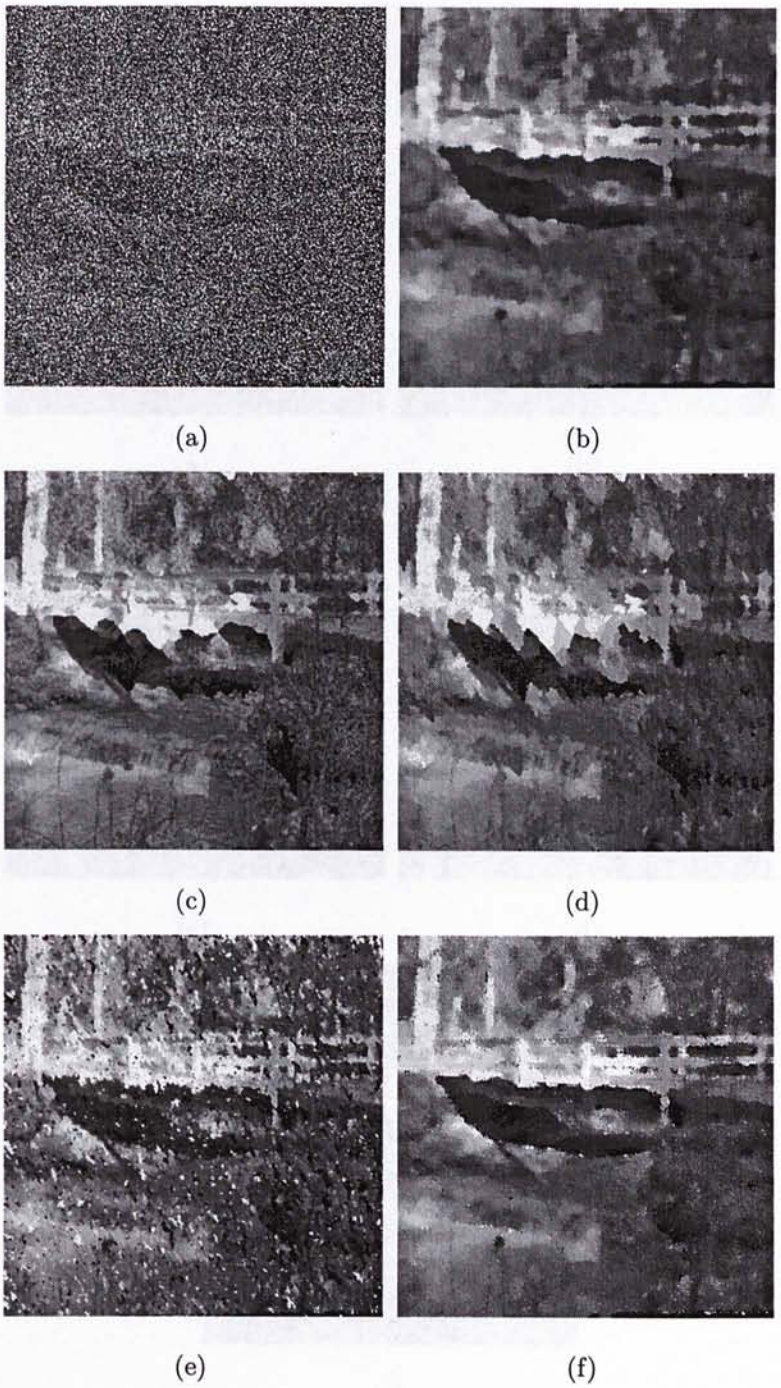

Figure 5: Restoration results of different filters: (a) Corrupted *Bridge* image with 70% salt-and-pepper noise (6.8 dB), (b) MED filer (19.8 dB), (c) PSM filter (17.0 dB), (d) MSM filter (16.4 dB), (e) DDBSM filter (15.9 dB), (f) NASM filter (19.9 dB)

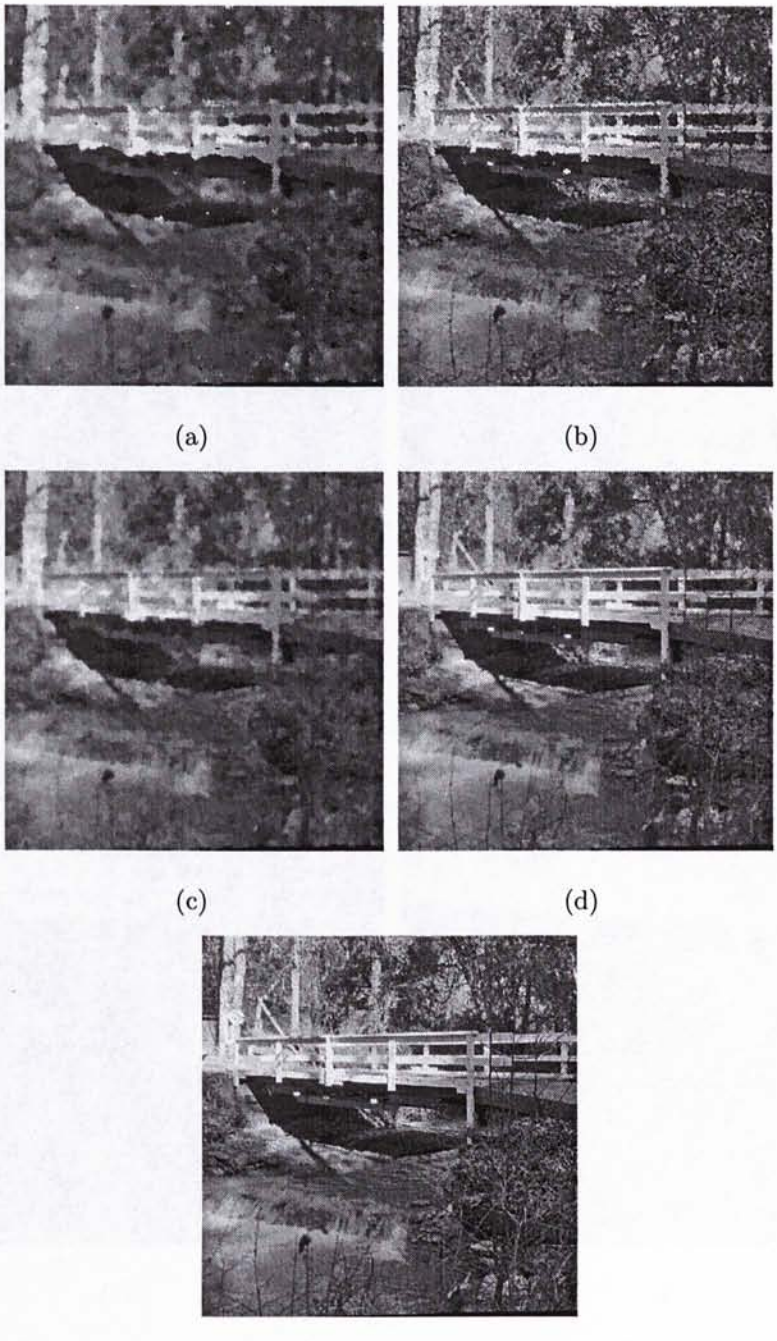

(a) (b) (c) (d) (e)

Figure 6: Restoration results of different filters: (a) ISM filter (20.1 dB), (b) Algorithm I (21.8 dB), (c) Algorithm II (21.1 dB), (d) Our proposed algorithm (25.0 dB), and (e) Original image.

(a) (b)

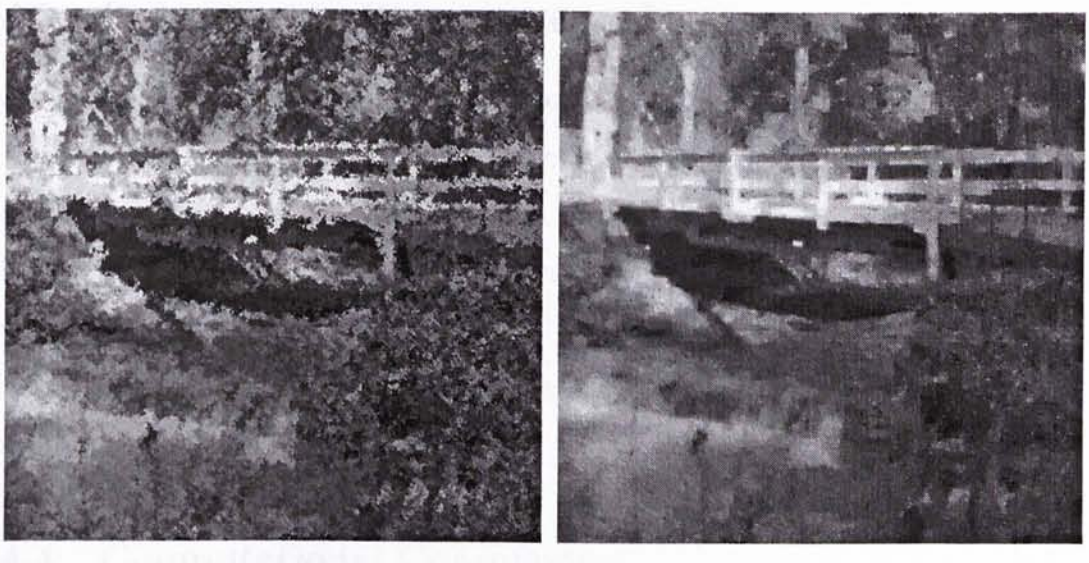

(c) (d)

Figure 7: Restorations of 90% corrupted images: (a) *Lena* by Algorithm I (21.1 dB), (b) *Lena* by Algorithm III (25.4 dB), (c) *Bridge* by Algorithm I (18.1 dB), and (d) *Bridge* by Algorithm III (21.5 dB).

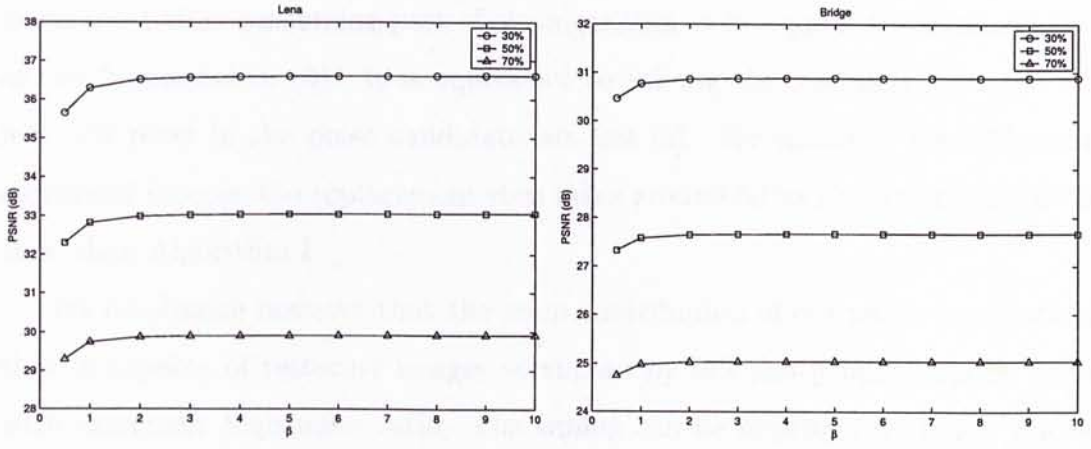

(a) (b)

Figure 8: PSNR of restored images by our Algorithm III for different β: (a) *Lena* image and (b) *Bridge* image.

4.3 Robustness with respect to β

For Algorithm II, the choice of β is crucial in the restoration. To show that our Algorithm III is robust with respect to β, $0.5 \leq \beta \leq 10$ are tested for noise levels 30%, 50% and 70%, see Figure 8. From the plots, we see that the PSNR is very stable when $1 \leq \beta \leq 10$. Hence one can set $\beta = 5$ for all denoising problems in practice. If one further use $\varphi(t) = |t|^{1.3}$ as we did in our tests, and set $w_{\max} = \min\{M, N\}$ (which will be able to detect all salt-and-pepper noise), then our algorithm is parameter free.

4.4 Computational Complexity

We end this section by considering the complexity of our algorithm. Our algorithm requires two phases: noise detection and replacement. Noise detection is done by Algorithm I. Like other median-type filters, Algorithm I can be processed very fast. Although $w_{\max}$ may be quite large, the loop in Algorithm I is automatically stopped at Step 3 when the noise level is not high. The replacement step

is the most time-consuming part of our algorithm as it requires the minimization of the functional in (3). It is equivalent to solving the nonlinear equation (2) for each pixel in the noise candidate set, see [5]. For example, for 50% noise corrupted images, the replacement step takes around 50 to 100 times more CPU time than Algorithm I.

We emphasize however that the main contribution of our paper is a method that is capable of restoring images corrupted by salt-and-pepper impulse noise with extremely high noise ratio. The timing can be improved by better implementations of minimization routines for solving (3). One can view our method as a post-processing procedure that improves the images obtained by fast algorithms such as Algorithm I.

5 Conclusion

In this paper, we propose a decision-based, details preserving restoration method. It is the ultimate filter for removing salt-and-pepper noise. Experimental results show that our method performs much better than median-based filters or the edge-preserving regularization methods. Even at a very high noise level ($\leq 90\%$), the texture, details and edges are preserved accurately. One can further improve our results by using different noise detectors and regularization functionals that are tailored to different types of images and noises. These extensions will be discussed in our future works.

References

[1] J. Astola and P. Kuosmanen, *Fundamentals of Nonlinear Digital Filtering.* Boca Raton, CRC, 1997.

[2] M. Black and A. Rangarajan, "On the unification of line processes, outlier rejection, and robust statistics with applications to early vision," *International Journal of Computer Vision*, 19 (1996), pp. 57–91.

[3] C. Bouman and K. Sauer, "On discontinuity-adaptive smoothness priors in computer vision," *IEEE Transactions on Pattern Analysis and Machine Intelligence*, 17 (1995), pp. 576–586.

[4] A. Bovik, *Handbook of Image and Video Processing*, Academic Press, 2000.

[5] R. H. Chan, C.-W Ho, and M. Nikolova, "Convergence of Newton's method for a minimization problem in impulse noise removal", *Journal of Computational Mathematics*, 22 (2004), pp. 168–177.

[6] T. F. Chan, H. M. Zhou, and R. H. Chan, "A continuation method for total variation denoising problems," *Proceedings of SPIE Symposium on Advanced Signal Processing: Algorithms, Architectures, and Implementations, ed. F. T. Luk*, 2563 (1995), pp. 314–325,

[7] T. F. Chan and S. Esedoḡlu, "Aspects of total variation regularized L^1 function approximation," Department of Mathematics, UCLA, CAM Report (04-07), 2004.

[8] P. Charbonnier, L. Blanc-Féraud, G. Aubert, and M. Barlaud, "Deterministic edge-preserving regularization in computed imaging," *IEEE Transactions on Image Processing*, 6 (1997), pp. 298–311.

[9] T. Chen and H. R. Wu, "Space variant median filters for the restoration of impulse noise corrupted images," *IEEE Transactions on Circuits and Systems II*, 48 (2001), pp. 784–789.

[10] H.-L. Eng and K.-K. Ma, "Noise adaptive soft-switching median filter," *IEEE Transactions on Image Processing*, 10 (2001), pp. 242–251.

[11] R. C. Gonzalez and R. E. Woods, *Digital Image Processing Second Edition*, Prentice Hall, 2001; and *Book Errata Sheet (July 31, 2003)*, http://www.imageprocessingbook.com/downloads/errata_sheet.htm.

[12] P. J. Green, "Bayesian reconstructions from emission tomography data using a modified EM algorithm," *IEEE Transactions on Medical Imaging*, MI-9 (1990), pp. 84–93.

[13] Y. Hashimoto, Y. Kajikawa and Y. Nomura, "Directional difference-based switching median filters," *Electronics and Communications in Japan*, 85 (2002), pp. 22–32.

[14] T. S. Huang, G. J. Yang, and G. Y. Tang, "Fast two-dimensional median filtering algorithm," *IEEE Transactions on Acoustics, Speech, and Signal Processing*, 1 (1979), pp. 13–18.

[15] H. Hwang and R. A. Haddad, "Adaptive median filters: new algorithms and results," *IEEE Transactions on Image Processing*, 4 (1995), pp. 499–502.

[16] M. Nikolova, "Minimizers of cost-functions involving nonsmooth data-fidelity terms. Application to the processing of outliers," *SIAM Journal on Numerical Analysis*, 40 (2002), pp. 965–994.

[17] M. Nikolova, "A variational approach to remove outliers and impulse noise," *Journal of Mathematical Imaging and Vision*, 20 (2004), pp. 99–120.

[18] T A. Nodes and N. C. Gallagher, Jr. "The output distribution of median type filters," *IEEE Transactions on Communications*, COM-32, 1984.

[19] G. Pok, J.-C. Liu, and A. S. Nair, "Selective removal of impulse noise based on homogeneity level information," *IEEE Transactions on Image Processing*, 12 (2003), pp. 85–92.

[20] C. R. Vogel and M. E. Oman, "Fast, robust total variation-based reconstruction of noisy, blurred images," *IEEE Transactions on Image Processing*, 7 (1998), pp. 813–824.

[21] Z. Wang and D. Zhang, "Progressive switching median filter for the removal of impulse noise from highly corrupted images," *IEEE Transactions on Circuits and Systems II*, 46 (1999), pp. 78–80.

[22] S. Zhang and M. A. Karim, "A new impulse detector for switching median filters," *IEEE Signal Processing Letters*, 9 (2002), pp. 360–363.

Paper II: Convergence of Newton's Method for a Minimization Problem in Impulse Noise Removal *

Abstract

Recently, two-phase schemes for removing salt-and-pepper and random-valued impulse noise are proposed in [6, 7]. The first phase uses decision-based median filters to locate those pixels which are likely to be corrupted by noise (noise candidates). In the second phase, these noise candidates are restored using a detail-preserving regularization method which allows edges and noise-free pixels to be preserved. As shown in [18], this phase is equivalent to solving a one-dimensional nonlinear equation for each noise candidate. One can solve these equations by using Newton's method. However, because of the edge-preserving term, the domain of convergence of Newton's method will be very narrow. In this paper, we determine the initial guesses for these equations such that Newton's method will always converge.

Keywords. Impulse noise denoising, Newton's method, Variational Method.

1 Introduction

Impulse noise is caused by malfunctioning pixels in camera sensors, faulty memory locations in hardware, or transmission in a noisy channel. Some of the pixels in

*Paper II is a joint work with Raymond H. Chan and Mila Nikolova.

the images could be corrupted by the impulse noise while the remaining pixels remain unchanged. There are two types of impulse noise: fixed-valued noise and random-valued noise. For images corrupted by fixed-valued noise, the noisy pixels can take only some of the values in the dynamic range, e.g. the maximum and the minimum values in the so-called salt-and-pepper noise model. In contrast, the noisy pixels in images corrupted by random-valued noise can take any random values in the dynamic range.

There are many works proposed to clean the noise, see for instance the schemes proposed in [2, 17, 1, 12, 13, 19, 18, 6, 7]. In particular, decision-based median filters are popular in removing impulse noise because of their good denoising power and computational efficiency, see [16, 15, 22, 9, 20, 14]. However, the blurring of details and edges are clearly visible when the noise level is high. In comparison, the detail-preserving variational method proposed in [18] used non-smooth data-fitting term along with edge-preserving regularization to restore the images. The variational method can keep the edges. But when removing noise patches—several noise pixels connecting each other, the distortion of some uncorrupted image pixels at the edges cannot be avoided. To overcome the drawbacks, the two-phase schemes recently proposed in [6, 7] combine decision-based median filters and the detail-preserving variational method to clean the noise.

The first phase in the methods proposed in [6, 7] is based on the adaptive median filter [15] or the adaptive center-weighted median filter [9] to first locate those pixels which are likely to be corrupted by noise (noise candidates). Because of computational efficiency of median filters, this phase can be processed in a short time. The second phase is to restore those noise candidates by variational method given in [18]. It is to minimize the objective functional consisting of a data-fitting term and an edge-preserving regularization term. It is equivalent to solving a system of nonlinear equations for those noise candidates. As shown in [18], the root finding can be done by relaxation, and it results in solving a one-dimensional nonlinear equation for each noise candidate. The presence of the

edge-preserving regularization term introduces difficulties in solving the equations because the nonlinear functions can have very large derivatives in some regions. In particular, the convergence domain can be very small if Newton's method is used. In this report, we give an algorithm to locate the initial guess such that Newton's method always converges.

The outline of this report is as follows. In §2, we review both two-phase denoising schemes proposed in [6] and [7] for cleaning impulse noises. The initial guess of Newton's method for solving nonlinear equations is discussed in §3. Numerical results and conclusions are presented in §4 and §5 respectively.

2 Review of 2-Phase Denoising Schemes

Let $\{x_{ij}\}_{i,j=1}^{M,N}$ be the gray level of a true image $\mathbf{x}$ at pixel location (i,j), and $[s_{\min}, s_{\max}]$ be the dynamic range of $\mathbf{x}$. Denote $\mathbf{y}$ the noisy image. The observed gray level at pixel location (i,j) is given by

$$y_{ij} = \begin{cases} r_{ij}, & \text{with probability } p, \\ x_{ij}, & \text{with probability } 1-p, \end{cases}$$

where p defines the noise level. In salt-and-pepper noise model, r_{ij} take either $s_{\min}$ or $s_{\max}$, i.e. $r_{ij} \in \{s_{\min}, s_{\max}\}$, see [15]. In random-valued noise model, $r_{ij} \in [s_{\min}, s_{\max}]$ are random numbers, see [9].

2.1 Cleaning salt-and-pepper noise

A two-phase scheme is proposed in [6] to remove salt-and-pepper noise. The first phase is to use the adaptive median filter (AMF) [15] to identify the noise candidates. Then the second phase is to restore those noise candidates by minimizing the objective functional proposed in [18] which consists of an ℓ_1 data-fitting term and an edge-preserving regularization term. The algorithm is as follows:

Algorithm I

1. *(Noise detection):* Apply AMF to the noisy image $\mathbf{y}$ to get the noise candidate set $\mathcal{N}$.

2. *(Refinement):* If the range of the noise is known, we can refine $\mathcal{N}$ to $\mathcal{N}_T$. For example,

$$\mathcal{N}_T = \mathcal{N} \cap \{(i,j) : \ s_{\min} \le y_{ij} \le s_{\min} + T \quad \text{or} \quad s_{\max} - T \le y_{ij} \le s_{\max}\},$$

where $T \ge 0$ is a threshold. Or we can choose T such that

$$\frac{|\mathcal{N}_T|}{M \times N} \approx p.$$

In the case of salt-and-pepper noise we can take T close to zero.

3. *(Restoration):* We restore all pixels in $\mathcal{N}_T$ by minimizing the convex objective functional $F_{\mathbf{y}}$:

$$F_{\mathbf{y}}(\mathbf{x}) = \sum_{(i,j)\in\mathcal{N}_T} |x_{ij} - y_{ij}| + \frac{\beta}{2}\Big(\sum_{(i,j)\in\mathcal{N}_T} \sum_{(m,n)\in\mathcal{V}_{ij}} \varphi_\alpha(x_{ij} - x_{mn}) + \sum_{(m,n)\in\mathcal{V}_{\mathcal{N}_T}} \sum_{(i,j)\in\mathcal{V}_{mn}\bigcap\mathcal{N}_T} \varphi_\alpha(y_{mn} - x_{ij})\Big), \quad (1)$$

where φ_α is an edge-preserving potential function, β is a regularization parameter, $\mathcal{V}_{ij}$ denotes the four closest neighbors of (i,j) not including (i,j), and $\mathcal{V}_{\mathcal{N}_T} = \left(\bigcup_{(i,j)\in\mathcal{N}_T} \mathcal{V}_{ij}\right) \setminus \mathcal{N}_T$. Also we let $\hat{x}_{ij} = y_{ij}$ for $(i,j) \notin \mathcal{N}_T$. The minimizer $\hat{\mathbf{x}}$ of (1), which is the restored image, is found by Algorithm A which will be given later.

As mentioned in [18], in order for the minimization method in Step 3 above to be convergent, the function φ_α should satisfy (i) $\varphi_\alpha \in \mathcal{C}^1$, and (ii) φ_α is strongly convex on any bounded intervals. Examples of edge-preserving functions φ_α that satisfy these requirements are:

$$\varphi_\alpha(t) = |t|^\alpha, \quad 1 < \alpha \le 2, \quad (2)$$

$$\varphi_\alpha(t) = 1 + \frac{|t|}{\alpha} - \log\left(1 + \frac{|t|}{\alpha}\right), \quad \alpha > 0, \tag{3}$$

$$\varphi_\alpha(t) = \log\left(\cosh\left(\frac{t}{\alpha}\right)\right), \quad \alpha > 0, \tag{4}$$

$$\varphi_\alpha(t) = \sqrt{\alpha + t^2}, \quad \alpha > 0, \tag{5}$$

see [10, 4, 5, 3, 8].

2.2 Cleaning random-valued noise

To clean the random-valued noise, an iterative two-phase scheme is proposed in [7]. The first phase is to use the adaptive center-weighted median filter (ACWMF) [9] to identify the noise candidates. Then the second phase is to restore those noise candidates by the same variational method proposed in [7]. These two phases are applied iteratively to the image. The basic idea of the method is that at the early iterations, we increase the thresholds in ACWMF so that it will only select pixels that are most likely to be noisy; and then they will be restored by the variational method. In the later iterations, the thresholds are decreased to include more noise candidates. The algorithm is as follows:

Algorithm II

1. Set $r = 0$. Initialize $\mathbf{y}^{(r)}$ to be the observed image $\mathbf{y}$.
2. Apply ACWMF with the thresholds $T_k^{(r)}$ to the image $\mathbf{y}^{(r)}$ to get the noise candidate set $\mathcal{M}^{(r)}$.
3. Let $\mathcal{N}^{(r)} = \bigcup_{l=0}^{r} \mathcal{M}^{(l)}$.
4. We restore all pixels in $\mathcal{N}^{(r)}$ by minimizing the same objective functional $F_{\mathbf{y}}$ in (1) over $\mathcal{N}^{(r)}$. The corresponding minimizer $\hat{\mathbf{x}}$ will be denoted by $\mathbf{y}^{(r+1)}$. Again the minimizer will be found by Algorithm A given below.
5. If $r \leq r_{\max}$, set $r = r + 1$ and go back to Step 2. Otherwise, output the restored image $\hat{\mathbf{x}} = \mathbf{y}^{(r_{\max}+1)}$.

In Step 2, the thresholds are of the form

$$T_k^{(r)} = s \cdot \mathrm{MAD}^{(r)} + \delta_k + 20(r_{\max} - r),$$

for $0 \le k \le 3$, $0 \le r \le r_{\max}$, and $0 \le s \le 0.6$. Here $[\delta_0, \delta_1, \delta_2, \delta_3] = [40, 25, 10, 5]$, and the robust estimate MAD denotes the "median of the absolute deviations from the median", see [11, 2], i.e.

$$\mathrm{MAD}^{(r)} = \mathrm{median}\left\{ \left| y_{i-u,j-v}^{(r)} - \widetilde{y}_{ij}^{(r)} \right| : -h \le u, v \le h \right\}$$

and

$$\widetilde{y}_{ij}^{(r)} = \mathrm{median}\left\{ y_{i-u,j-v}^{(r)} : -h \le u, v \le h \right\},$$

where $(2h+1)$ defines the window length. In practice, $r_{\max} = 3$ is enough for satisfactory results.

The minimization algorithm in Step 3 of Algorithm I and in Step 4 of Algorithm II is given in [18]. It is a Jacobi-type relaxation algorithm and works on the residual $\mathbf{z} = \mathbf{x} - \mathbf{y}$. For convenience, let $\mathcal{P}$ be $\mathcal{N}_T$ in Step 3 of Algorithm I or $\mathcal{N}^{(r)}$ in Step 4 of Algorithm II. We restate the minimization algorithm in [18] as follows.

Algorithm A (Minimization Scheme)

1. Initialize $z_{ij}^{(0)} = 0$ for each (i, j) in the noise candidate set $\mathcal{P}$.
2. At each iteration k, do the following for each $(i, j) \in \mathcal{P}$:
   (a) Calculate
   $$\xi_{ij}^{(k)} = \beta \sum_{(m,n) \in \mathcal{V}_{ij}} \varphi_\alpha'(y_{ij} - z_{mn} - y_{mn}),$$
   where z_{mn}, for $(m, n) \in \mathcal{V}_{ij}$, are the latest updates and φ_α' is the derivative of φ_α.

(b) If $|\xi_{ij}^{(k)}| \leq 1$, set $z_{ij}^{(k)} = 0$. Otherwise, find $z_{ij}^{(k)}$ by solving the nonlinear equation

$$\beta \sum_{(m,n)\in\mathcal{V}_{ij}} \varphi'_\alpha(z_{ij}^{(k)} + y_{ij} - z_{mn} - y_{mn}) = \operatorname{sgn}(\xi_{ij}^{(k)}). \tag{6}$$

3. Stop the iteration when

$$\max_{i,j}\{|z_{ij}^{(k+1)} - z_{ij}^{(k)}|\} \leq \tau_A \quad \text{and} \quad \frac{F_{\mathbf{y}}(\mathbf{y}+\mathbf{z}^{(k)}) - F_{\mathbf{y}}(\mathbf{y}+\mathbf{z}^{(k+1)})}{F_{\mathbf{y}}(\mathbf{y}+\mathbf{z}^{(k)})} \leq \tau_A,$$

where τ_A is some given tolerance.

It was shown in [18] that the solution $z_{ij}^{(k)}$ of (6) satisfies

$$\operatorname{sgn}(z_{ij}^{(k)}) = -\operatorname{sgn}(\xi_{ij}^{(k)}), \tag{7}$$

and that $\mathbf{z}^{(k)}$ converges to $\hat{\mathbf{z}} = \hat{\mathbf{x}} - \mathbf{y}$ where $\hat{\mathbf{x}}$ is the minimizer for (1).

3 Algorithm for Solving (6)

It is well-known that the edges and details are preserved better if the potential function $\varphi_\alpha(t)$ is close to $|t|$—the celebrated TV norm function developed in [21]. For φ_α in (2), this means that α should be chosen close to 1. For φ_α in (3)–(5), we should choose α close to 0. Notice that all φ'_α will have a steep increase near zero and that φ''_α will have a large value at zero—in fact it is infinite for φ_α in (2). The function (6) therefore will have very large slopes in some regions which makes the minimization difficult. Although Newton's minimization is preferable to speed up the convergence, its use is delicate since the convergence domain can be very narrow. In this section we discuss how to find the initial guess such that Newton's method is guaranteed to converge. We will focus on how to solve (6) when $\varphi_\alpha(t) = |t|^\alpha$ with $\alpha > 1$. With some modifications, similar techniques can be applied to other edge-preserving φ_α too.

According to Step 2(b) of Algorithm A, we only need to solve (6) if $|\xi_{ij}^{(k)}| > 1$. We first consider the case where $\xi_{ij}^{(k)} > 1$. When solving (6), $z_{mn} + y_{mn} - y_{ij}$, for

$(m,n) \in \mathcal{V}_{ij}$, are known values. Let these values be denoted by d_j, for $1 \le j \le 4$, and be arranged in an increasing order: $d_j \le d_{j+1}$. Then (6) can be rewritten as

$$H(z) \equiv -1 + \alpha\beta \sum_{j=1}^{4} \operatorname{sgn}(z - d_j)|z - d_j|^{\alpha-1} = 0. \tag{8}$$

Since each term inside the summation sign above is a strictly increasing function on $\mathbb{R}$, $H(z)$ is a strictly increasing function on $\mathbb{R}$. Clearly $H(d_1) < 0$ and $\lim_{z\to\infty} H(z) = \infty$. Hence (8) has a unique solution $z^* > d_1$. By evaluating $\{H(d_j)\}_{j=2}^4$, we can check that if any one of the d_j, $2 \le j \le 4$, is the root z^*. If not, then z^* lies in one of the following intervals:

$$(d_1, d_2), (d_2, d_3), (d_3, d_4), \text{or } (d_4, \infty), \tag{9}$$

We first consider the case where z^* is in one of the finite intervals (d_j, d_{j+1}). For simplicity, we give the details only for the case where $z^* \in (d_2, d_3)$. The other cases can be analyzed similarly.

Let $z^* \in (d_2, d_3)$, i.e. $H(d_2) < 0$ and $H(d_3) > 0$. Then we compute $H\left(\frac{d_2+d_3}{2}\right)$. Without loss of generality, let us assume that $H\left(\frac{d_2+d_3}{2}\right) > 0$. Our aim is to find an initial guess $z^{(0)} \in [d_2, (d_2+d_3)/2)$ with $H(z^{(0)}) \le 0$. Unfortunately, we cannot use d_2 as the initial guess as $H'(d_2)$ is undefined. We will prove in Theorem 2 that Newton's method with $z^{(0)} \equiv d_2 + \varepsilon$ can solve (8), where $\varepsilon > 0$ is given below.

Lemma 1. *Let*

$$\varepsilon \equiv \left[\frac{-H(d_2)}{4\alpha\beta}\right]^{\frac{1}{\alpha-1}}. \tag{10}$$

Then $H(d_2 + \varepsilon) \le 0$. As a result, $z^* \in [d_2 + \varepsilon, (d_2 + d_3)/2)$.

Proof. First let $\tilde{\varepsilon} = \min\{(d_3 - d_2)/2, \varepsilon\} > 0$. By (8), we have

$$H(d_2+\tilde{\varepsilon}) = -1+\alpha\beta\Big[(d_2-d_1+\tilde{\varepsilon})^{\alpha-1}+\tilde{\varepsilon}^{\alpha-1}-(d_3-d_2-\tilde{\varepsilon})^{\alpha-1}-(d_4-d_2-\tilde{\varepsilon})^{\alpha-1}\Big].$$

For $1 < \alpha \le 2$, we can easily verify the inequalities:

$$(c+\delta)^{\alpha-1} \le c^{\alpha-1} + \delta^{\alpha-1}, \quad \text{for all } c, \delta \ge 0,$$

$$(c-\delta)^{\alpha-1} \geq c^{\alpha-1} - \delta^{\alpha-1}, \quad \text{for all } c \geq \delta \geq 0.$$

Since $\tilde{\varepsilon} \leq (d_3 - d_2)/2 < (d_3 - d_2) \leq (d_4 - d_2)$, we obtain

$$\begin{aligned} H(d_2 + \tilde{\varepsilon}) &\leq -1 + \alpha\beta\Big\{(d_2 - d_1)^{\alpha-1} + \tilde{\varepsilon}^{\alpha-1} + \tilde{\varepsilon}^{\alpha-1} - [(d_3 - d_2)^{\alpha-1} - \tilde{\varepsilon}^{\alpha-1}] \\ &\quad -[(d_4 - d_2)^{\alpha-1} - \tilde{\varepsilon}^{\alpha-1}]\Big\} \\ &= H(d_2) + 4\alpha\beta\tilde{\varepsilon}^{\alpha-1}. \end{aligned}$$

By (10), we have

$$H(d_2 + \tilde{\varepsilon}) \leq H(d_2) + 4\alpha\beta\tilde{\varepsilon}^{\alpha-1} \leq H(d_2) + 4\alpha\beta\varepsilon^{\alpha-1} = 0.$$

However, because $H((d_2 + d_3)/2) > 0$ and H is strictly increasing, we must have $\tilde{\varepsilon} < (d_3 - d_2)/2$. As a result, $\tilde{\varepsilon} = \varepsilon$ and $H(d_2 + \varepsilon) \leq 0$. □

Theorem 2. *Let $z^{(0)} = d_2 + \varepsilon$ be the initial guess where ε is defined in (10). Then the sequence generated by Newton's method, i.e.*

$$z^{(n+1)} = z^{(n)} - \frac{H(z^{(n)})}{H'(z^{(n)})}, \tag{11}$$

converges to the root z^* of $H(z)$.

Proof. Consider the Taylor expansion of $H(z)$ at $z = z^*$. We have

$$H(z) = H(z^*) + (z - z^*)H'(\tilde{z}) = (z - z^*)H'(\tilde{z}),$$

where $\tilde{z}$ lies strictly between z and z^*. Hence by (11),

$$z^* - z^{(n+1)} = \left(1 - \frac{H'(\tilde{z}^{(n)})}{H'(z^{(n)})}\right)(z^* - z^{(n)}), \tag{12}$$

where $\tilde{z}^{(n)}$ lies strictly between $z^{(n)}$ and z^*. We note that $d_2 < z^{(0)} < \tilde{z}^{(0)} < z^* < (d_2 + d_3)/2$.

We need the following facts to complete the proof:

F1. Clearly from the definition (8), $H'(z) = \alpha(\alpha-1)\beta\sum_{j=1}^{4}|z - d_j|^{\alpha-2} > 0$ for all $z \in (d_2, d_3)$.

F2. Since $H'''(z) = \alpha(\alpha-1)(\alpha-2)(\alpha-3)\beta\sum_{j=1}^{4}|z-d_j|^{\alpha-4} > 0$ for all $z \in (d_2, d_3)$, $H''(z)$ is strictly increasing in (d_2, d_3).

F3. Define $W(z) \equiv \alpha(\alpha-1)\beta\sum_{j=2}^{3}|z-d_j|^{\alpha-2}$. Clearly $W(z) < H'(z)$ for all z. Moreover, $W'(z) < 0$ for $z \in (d_2, (d_2+d_3)/2)$. Hence $W(z)$ is a strictly decreasing function in $(d_2, (d_2+d_3)/2)$.

We divide the convergence proof in two cases:

(i) $H''(z^*) \le 0$: F2 implies that $H''(z) < 0$ in (d_2, z^*). Hence $H'(z)$ is decreasing in (d_2, z^*). Therefore, $H'(\tilde{z}) \le H'(z)$ for $d_2 < z < \tilde{z} < z^*$. Together with F1, we have

$$0 \le 1 - \frac{H'(\tilde{z})}{H'(z)} < 1, \qquad \text{for all } d_2 < z < \tilde{z} < z^*.$$

Therefore, from (12), we have

$$0 \le z^* - z^{(n+1)} < z^* - z^{(n)}, \quad n = 0, 1, \ldots,$$

i.e. the sequence $\{z^{(n)}\}$ converges monotonically to z^* from the left.

(ii) $H''(z^*) > 0$: For all $z \in (d_2, (d_2+d_3)/2)$, since

$$|z-d_1|^{\alpha-2} \le |z-d_2|^{\alpha-2} \quad \text{and} \quad |z-d_4|^{\alpha-2} \le |z-d_3|^{\alpha-2},$$

we have

$$H'(z) \le 2\alpha(\alpha-1)\beta\sum_{j=2}^{3}|z-d_j|^{\alpha-2} = 2W(z), \qquad \text{for all } z \in (d_2, (d_2+d_3)/2).$$

Here $W(z)$ is defined in F3. Since $W(z)$ is a strictly decreasing function in $(d_2, (d_2+d_3)/2)$ and $W(z) < H'(z)$ for all z, we have

$$H'(\tilde{z}) \le 2W(\tilde{z}) \le 2W(z) < 2H'(z), \qquad \text{for all } d_2 < z < \tilde{z} < z^*.$$

Hence

$$\left|1 - \frac{H'(\tilde{z})}{H'(z)}\right| < 1, \qquad \text{for all } d_2 < z < \tilde{z} < z^*.$$

Therefore by (12), as long as $d_2 < z^{(n)} < z^*$, we have

$$|z^* - z^{(n+1)}| < |z^* - z^{(n)}|,$$

i.e. the sequence $\{z^{(n)}\}$ converges to z^* as long as $z^{(n)} < z^*$ for all n.

But what if after some iterations, $z^{(m)} > z^*$? Since $H''(z^*) > 0$, by F2, we have $H''(z) > 0$ in $[z^*, d_3)$. This implies that $H'(z)$ is increasing in $[z^*, d_3)$. As a result, $H'(\tilde{z}) \leq H'(z)$ for all $z^* < \tilde{z} < z$. Therefore,

$$0 \leq 1 - \frac{H'(\tilde{z})}{H'(z)} < 1, \qquad \text{for all } z^* < \tilde{z} < z.$$

Hence, from (12), we have

$$0 \leq z^{(n+1)} - z^* < z^{(n)} - z^*, \quad n = m, m+1, \ldots,$$

i.e. the sequence $\{z^{(n)}\}_{n=m}^{\infty}$ converges monotonically to z^* from the right.

□

This finishes the proof for the case when $H\left(\frac{d_2+d_3}{2}\right) > 0$. If $H\left(\frac{d_2+d_3}{2}\right) < 0$, then we locate $z^{(0)} \in ((d_2 + d_3)/2, d_3]$. More precisely, $z^{(0)} = d_3 - \varepsilon$ with $\varepsilon = [H(d_3)/(4\alpha\beta)]^{\frac{1}{\alpha-1}}$. The rest of the proof will be similar.

The same result holds when z^* lies in other finite intervals (d_j, d_{j+1}), $j = 1, 2, 3$. If $H(d_4) < 0$, this means $z^* \in (d_4, \infty)$. Since

$$H''(z) = \alpha(\alpha-1)(\alpha-2)\beta \sum_{j=1}^{4} \operatorname{sgn}(z - d_j)|z - d_j|^{\alpha-3} < 0, \qquad \text{for all } z \in (d_4, \infty),$$

we are in a situation similar to case (i) in Theorem 2. In fact, as $H'(z)$ is strictly decreasing in (d_4, ∞), $0 < 1 - H'(\tilde{z})/H(z) < 1$ for all $d_4 < z < \tilde{z} < z^*$. Therefore it suffice to choose an initial guess $z^{(0)} = d_4 + \varepsilon$ such that $H(z^{(0)}) < 0$. (Again we cannot choose $z^{(0)} = d_4$ as $H'(d_4)$ is undefined.) Similar to Lemma 1, we can choose $\varepsilon = [-H(d_4)/(4\alpha\beta)]^{\frac{1}{\alpha-1}}$. Then one can show from (12) that $0 \leq z^* - z^{(n+1)} < z^* - z^{(n)}$, for $n = 0, 1, \ldots$, i.e. $\{z^{(n)}\}$ converges monotonically to z^* from the left.

We remark that since we are considering the case that $\xi_{ij}^{(k)} > 1$, by (7), $\mathrm{sgn}(z^*) = -\mathrm{sgn}(\xi_{ij}^{(k)}) = -1$. Hence $z^* < 0$. Thus we may not need to check all the intervals in (9) for z^*. In fact, if $d_\ell < 0 < d_{\ell+1}$, then we only have to check the intervals $\{(d_j, d_{j+1})\}_{j=1}^{\ell}$. This can simplify the algorithm (see Step 1 in Algorithm B below).

Finally, we turn to the case where $\xi_{ij}^{(k)} < -1$. The nonlinear equation in (8) becomes:

$$1 + \alpha\beta \sum_{j=1}^{4} \mathrm{sgn}(z - d_j)|z - d_j|^{\alpha-1} = 0,$$

where the left-hand-side function is still a strictly increasing function in z, and that $z^* > 0$ by (7). The convergence proof is almost the same with minor modifications.

We summarize the results into the following algorithm. It works for both $\xi_{ij}^{(k)} > 1$ and $\xi_{ij}^{(k)} < -1$.

Algorithm B (Newton's Solver for Solving (6))

1. Check the signs of $H(d_j)$, $1 \le j \le 4$. (One may not need to check all four points by taking into account the sign of z^* using (7).)

2. If $H(d_1) > 0$ or $H(d_4) < 0$, let

$$z^{(0)} = \begin{cases} d_1 - \left\{ \dfrac{H(d_1)}{4\alpha\beta} \right\}^{\frac{1}{\alpha-1}}, & \text{if } H(d_1) > 0, \\ d_4 + \left\{ -\dfrac{H(d_4)}{4\alpha\beta} \right\}^{\frac{1}{\alpha-1}}, & \text{if } H(d_4) < 0. \end{cases}$$

3. Else locate the interval (d_j, d_{j+1}) which contains the root z^*, and let

$$z^{(0)} = \begin{cases} d_{j+1} - \left\{ \dfrac{H(d_{j+1})}{4\alpha\beta} \right\}^{\frac{1}{\alpha-1}}, & \text{if } H\left(\dfrac{d_j + d_{j+1}}{2} \right) < 0, \\ d_j + \left\{ -\dfrac{H(d_j)}{4\alpha\beta} \right\}^{\frac{1}{\alpha-1}}, & \text{if } H\left(\dfrac{d_j + d_{j+1}}{2} \right) > 0. \end{cases}$$

4. Apply Newton's method to obtain z^* up to a given tolerance τ_B.

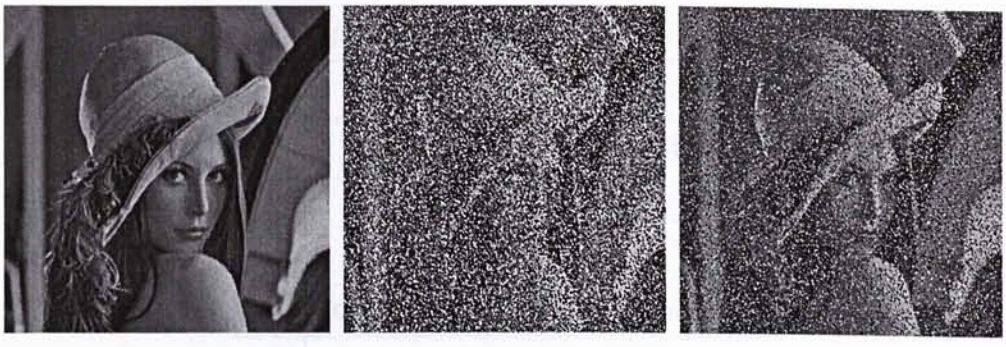

Figure 1: (Left) The original Lena image. (Middle) The noisy image corrupted with 50% salt-and-pepper noise. (Right) The noisy image corrupted with 40% random-valued noise.

4 Numerical Results

In this section, we stimulate the restoration of the 256-by-256 gray scale image *Lena* corrupted by 50% salt-and-pepper noise and 40% random-valued impulse noise with dynamic range $[0, 255]$, see Figure 1. Here the salt noise (i.e. $s_{\max}$) and the pepper noise (i.e. $s_{\min}$) are of equal probability and the random-valued noise are uniformly distributed in the dynamic range. We clean the salt-and-pepper noise by Algorithm I with threshold $T = 5$ and the random-valued noise by Algorithm II with $s = 0.1$. In both algorithms, we use windows of size 9-by-9 for noise detection.

We test our Newton's method with different magnitudes of α and choose $\beta = 2$ for all settings. The tolerances in Algorithms A and B are chosen to be $\tau_A = (s_{\max} - s_{\min}) \times 10^{-4}$ and $\tau_B = 5 \times 10^{-4}$ respectively. In Table 1, we give, for different values of α, the maximum number of inner iterations (i.e. maximum number of Newton's iterations in Step 4 of Algorithm B), and the total number of outer iterations (i.e. maximum k in Algorithm A).

From the table, we see that around 5 to 9 iterations are sufficient for Newton's method to converge. The smaller α is, the more iterations $|t|^\alpha$ requires. But in practice, there will be stair-case effects in the restored image if α is too small.

α	inner iterations	outer iterations
1.3	5	117
1.2	6	201
1.1	9	290

α	inner iterations	outer iterations
1.3	5	319
1.2	6	512
1.1	9	1208

Table 1: The number of iterations in restoring noisy image corrupted by (top) salt-and-pepper noise and (bottom) random-valued noise.

To restore the best image, $1.25 \leq \alpha \leq 1.40$ is sufficient. We give the restored images in Figure 2. We see that the noise are successfully suppressed while the edges and details are well preserved.

5 Conclusions

In this report, we first give an overview of denoising schemes for cleaning salt-and-pepper and random-valued impulse noise. Experimental results show that the images are restored satisfactory even at very high noise level. Then we present an algorithm for solving the variational equations resulting from the denoising schemes. It is the essential step in the restoration process. To overcome the difficulty in finding the convergence domain, we have derived a formula for the initial guess; and proved that with it, Newton's method is guaranteed to converge.

Figure 2: (Left) Restoration from image corrupted by salt-and-pepper noise using $\alpha = 1.3$ and $\beta = 2.5$. (Right) Restoration from image corrupted by random-valued noise using $\alpha = 1.3$ and $\beta = 2.3$.

References

[1] G. R. Arce and R. E. Foster, "Detail-preserving ranked-order based filters for image processing," *IEEE Transactions on Acoustics, Speech, and Signal Processing*, 37 (1989), pp. 83–98.

[2] J. Astola and P. Kuosmanen, *Fundamentals of Nonlinear Digital Filtering.* Boca Raton, CRC, 1997.

[3] M. Black and A. Rangarajan, "On the unification of line processes, outlier rejection, and robust statistics with applications to early vision," *International Journal of Computer Vision*, 19 (1996), pp. 57–91.

[4] C. Bouman and K. Sauer, "A generalized Gaussian image model for edge-preserving MAP estimation," *IEEE Transactions on Image Processing*, 2 (1993), pp. 296–310.

[5] C. Bouman and K. Sauer, "On discontinuity-adaptive smoothness priors in computer vision," *IEEE Transactions on Pattern Analysis and Machine Intelligence*, 17 (1995), pp. 576–586.

[6] R. H. Chan, C.-W. Ho, and M. Nikolova, "Impulse noise removal by median-type noise detectors and edge-preserving regularization," *Report*, Department of Mathematics, The Chinese University of Hong Kong, 2003-28 (302).

[7] R. H. Chan, C. Hu, and M. Nikolova, "An iterative procedure for removing random-valued impulse noise," *Report*, Department of Mathematics, The Chinese University of Hong Kong, 2003-33 (307).

[8] P. Charbonnier, L. Blanc-Féraud, G. Aubert, and M. Barlaud, "Deterministic edge-preserving regularization in computed imaging," *IEEE Transactions on Image Processing*, 6 (1997), pp. 298–311.

[9] T. Chen and H. R. Wu, "Space variant median filters for the restoration of impulse noise corrupted images," *IEEE Transactions on Circuits and Systems II*, 48 (2001), pp. 784–789.

[10] P. J. Green, "Bayesian reconstructions from emission tomography data using a modified EM algorithm," *IEEE Transactions on Medical Imaging*, MI-9 (1990), pp. 84–93.

[11] F. R. Hampel, E. M. Ronchetti, P. J. Rousseeuw, and W. A. Stahel, *Robust statistics: The Approach based on influence functions*, New York: Wiley, 1986.

[12] W.-Y. Han and J.-C. Lin, "Minimum-maximum exclusive mean (MMEM) filter to remove impulse noise from highly corrupted images," *Electronics Letters*, 33 (1997), pp. 124–125.

[13] R. C. Hardie and K. E. Barner, "Rank conditioned rank selection filters for signal restoration," *IEEE Transactions on Image Processing*, 3 (1994), pp. 192–206.

[14] T. S. Huang, G. J. Yang, and G. Y. Tang, "Fast two-dimensional median filtering algorithm," *IEEE Transactions on Acoustics, Speech, and Signal Processing*, 1 (1979), pp. 13–18.

[15] H. Hwang and R. A. Haddad, "Adaptive median filters: new algorithms and results," *IEEE Transactions on Image Processing*, 4 (1995), pp. 499–502.

[16] S.-J. Ko and Y. H. Lee, "Center weighted median filters and their applications to image enhancement," *IEEE Transactions on Circuits and Systems*, 38 (1991), pp. 984–993.

[17] Y. H. Lee and S. A. Kassam, "Generalized median filtering and related nonlinear filtering techniques," *IEEE Transactions on Acoustics, Speech, and Signal Processing*, 33 (1985), pp. 672–683.

[18] M. Nikolova, "A variational approach to remove outliers and impulse noise," *Journal of Mathematical Imaging and Vision*, 20 (2004), pp. 99–120.

[19] I. Pitas and A. Venetsanopoulos, "Nonlinear mean filters in image processing," *IEEE Transactions on Acoustics, Speech, and Signal Processing*, 34 (1986), pp. 600–609.

[20] G. Pok, J.-C. Liu, and A. S. Nair, "Selective removal of impulse noise based on homogeneity level information," *IEEE Transactions on Image Processing*, 12 (2003), pp. 85–92.

[21] L. Rudin, S. Osher, and E. Fatemi, "Nonlinear total variation based noise removal algorithms," *Physica D*, 60 (1992), pp. 259–268.

[22] T. Sun and Y. Neuvo, "Detail-preserving median based filters in image processing," *Pattern Recognition Letters*, 15 (1994), pp. 341–347.

Concluding Remark

We have developed a powerful method for denoising impulse noise. It is a two-phase method. In phase one, a suitable median-type filter, tailored to a priori known noise model such as salt-and-pepper noise or random-valued noise, will be chosen to locate the noise accurately. Then the detected noise will be removed in phase two by a recently proposed regularization method which is equipped with ℓ_1-norm data-fidelity term. Numerical results have shown that the second phase is much better than those methods which just use median values to replace the noise pixels. Practically, the proposed denoising method is equivalent to solving nonlinear equations iteratively and this can be solved by Newton's method with the derived initial guess to achieve quadratic convergence. As a result, this two-phase denoising scheme may be a first practical method to restored highly corrupted images, even when the noise level is as high as 90%.